Robotica (2011) volume 29, pp. 657–665. © Cambridge University Press 2010
doi:10.1017/S0263574710000512

Stable running of a planar underactuated biped robot

Yong Hu, Gangfeng Yan and Zhiyun Lin*

College of Electrical Engineering, Zhejiang University, 38 Zheda Road, Hangzhou, 310027 P. R. China

(Received in Final Form: August 5, 2010. First published online: September 1, 2010)

SUMMARY

This paper investigates the stable-running problem of a planar underactuated biped robot, which has two springy telescopic legs and one actuated joint in the hip. After modeling the robot as a hybrid system with multiple continuous state spaces, a natural passive limit cycle, which preserves the system energy at touchdown, is found using the method of *Poincaré* shooting. It is then checked that the passive limit cycle is not stable. To stabilize the passive limit cycle, an event-based feedback control law is proposed, and also to enlarge the basin of attraction, an additive passivity-based control term is introduced only in the stance phase. The validity of our control strategies is illustrated by a series of numerical simulations.

KEYWORDS: Biped robot; Passive running; Underactuated system.

1. Introduction

The idea of running robots with one leg, commonly called hoppers, was firstly proposed by Raibert[26] and Raibert and Tello.[27] Under proper initial conditions, the spring-driven one-legged hopping robot can hop periodically without external inputs. However, the periodic orbit may not be stable. Recently, to stabilize the running motion of hoppers, several control schemes are introduced.[3,28,32] The control for hoppers is usually decomposed into three components to regulate the hopping height, the touchdown leg angle, and the body attitude. Similar control strategies are also used to achieve stable running for quadrupedal robots.[25,26]

In addition to the interest on one-legged robots or quadrupedal robots, biped robots attract much more attentions. There appear many successful demonstrations of stable running of bipedal robots with revolute knees.[8,16,19,21,29] The earlier works mainly concerned the zero moment point, based on which many prototype 3-D bipedal robots were built all over the world such as QRIO[13,17] by Sony, ASIMO[15] by Honda, and HRP-2[18] by the AIST and Kawada Industries. They have succeeded in running experiments. Nevertheless, high computational cost and large energy consumption are always a big issue using this method. Moreover, it is very difficult to provide rigorous analysis for the system behavior. Recently, feedback control design is adopted, which leads to the notion of hybrid zero dynamics for running and allows stability analysis for running gaits. Using the idea, optimal-cyclic open-loop running trajectories for the five-link, four-actuator bipedal robot RABBIT are obtained in ref. [5]. The design of the prototype and related technological considerations are described in refs. [4, 7]. Further work about asymptotical stable running of RABBIT is reported in refs. [8, 9]. On the other hand, for the energy saving issue, Hyon and Emura[16] extend the running controller for passive one-legged hoppers to a planar biped robot with torso and two hip actuators, where the controller is derived based on energy-preserving strategies. In addition, Owaki and Ishiguro[22] and Owaki *et al.*[23] investigate how the body properties influence the passive running motion on a slope. Passive running is a direct extension of the successful idea of passive walking, which is pioneered by McGeer more than a decade ago[20] and has been widely studied in recent years.[1,10–12,14,31] The passive gait is helpful to explain the efficiency of human bipedal locomotion. To some extent, passive running offers the same principle as passive walking though the dynamic models are different even for the same robot.

Motivated by the recent progress in the field based on the ideas of passive running and feedback control design, we study the problem of achieving a stable running motion for a planar underactuated biped robot by stabilizing a passive limit cycle. The goal is to reduce energy consumption by regulating the running gait to a passive limit cycle. The robot we considered has two telescopic legs and only one actuated joint in the hip. We first derive the dynamic model for the robot, represented by a hybrid system with multiple continuous state spaces. For that, we look for a natural passive limit cycle that preserves the system energy at touchdown. That is, when the periodic running motion of the robot is exactly the passive limit cycle, ideally no energy is consumed at all. However, by looking at the *Poincaré* map, it is obtained that the passive limit cycle is not stable. Hence, in the paper an event-based feedback control law is presented to stabilize the passive limit cycle. Thus, with an appropriate initial state nearby the passive limit cycle, the periodic orbit of the running motion asymptotically converges to the passive limit cycle under our proposed control law that is piecewise constant. Also, in order to enlarge the basin of attraction, an additive passivity-based control term, which is a continuous feedback ensuring that the trajectory asymptotically converge to the passive limit cycle in the stance phase, is proposed. The stable running behavior and the basin of attraction are shown and demonstrated by simulations. A similar problem was

* Corresponding author. E-mail: linz@zju.edu.cn

https://doi.org/10.1017/S0263574710000512 Published online by Cambridge University Press

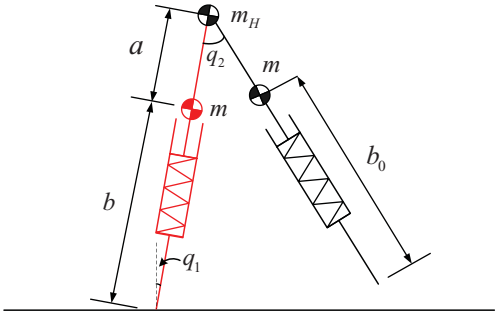


Fig. 1. The schematic structure.

Table I. Parameters of the robot.

Parameters used in simulations	
m	5 kg
m_H	10 kg
a	0.5 m
b_0	0.8 m
l	$a+b$
l_0	$a+b_0$
K_s	1000 N/m
g	9.8 m/s^2

studied in ref. [16] based on energy-preserving strategies, where a running controller for passive one-legged hoppers is extended to a planar biped with a torso and two hip actuators. However, different from our result, the running motion is still energy consuming even on the desired periodic orbit.

2. Dynamic model of a running robot

The robot we investigate in this paper is a planar underactuated biped robot, which has two springy telescopic legs and one actuated joint at the hip. Figure 1 shows the schematic structure of the planar bipedal robot. The mass of the robot is assumed to concentrate at three points: a hip mass m_H and two leg masses $m_1 = m_2 = m$. The length of the uncompressed spring is b_0, while b represents its current length. We define two angles q_1 and q_2 (see Fig. 1) where q_1 is the rotated angle of the stance leg relative to the vertical line and q_2 is the rotated angle of the swing leg relative to the stance leg. Clockwise rotation is considered negative and counterclockwise rotation as positive. The position of its center of gravity (CoG) is denoted by $(x_{cm}, y_{cm}) \in \mathbb{R}^2$. Table I lists the values of the parameters used in later simulations.

A running motion is composed of consecutive stance phases, flight phases, and state transitions from one phase to the other (see Fig. 2). We assume that there is no rebound and no slipping when landing. Also, we assume that the springs are mass less and do not cause any energy consumption. In the following, we show the equations of motion at each phase in an abbreviated form. The details on modeling a bipedal running motion can be found in ref. [33].

2.1. Stance-phase model

Denote $\mathbf{q_s} = [q_1\ q_2\ b]^T$ the configuration of the robot at the stance phase. The Lagrangian function is given by

$$L(\mathbf{q_s}, \dot{\mathbf{q}}_\mathbf{s}) = K(\mathbf{q_s}, \dot{\mathbf{q}}_\mathbf{s}) - V(\mathbf{q_s})$$

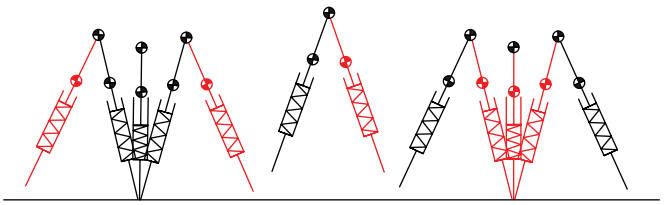


Fig. 2. A running motion: stance, takeoff, flight, and touchdown.

where

$$K(\mathbf{q_s}, \dot{\mathbf{q}}_\mathbf{s}) = \frac{1}{2}\dot{\mathbf{q}}_\mathbf{s}^\mathbf{T}\mathbf{D_s}(\mathbf{q_s})\dot{\mathbf{q}}_\mathbf{s}$$

is the total kinetic energy and $V(\mathbf{q_s})$ is the total potential energy. Note that for the robot shown in Fig. 1, $\mathbf{D_s}(\mathbf{q_s})$ is symmetric positive definite and does not depend on the state q_1. The total potential energy $V(\mathbf{q_s})$ of the robot can be expressed as

$$V(\mathbf{q_s}) = (2m + m_H)g y_{cm} + \frac{1}{2}K_s(b - b_0)^2$$

where y_{cm} is the CoG and it is a function of $\mathbf{q_s}$, b_0 is the natural spring length, and K_s is the spring rate. Applying the Lagrangian method, the dynamics at the stance phase is given as

$$\mathbf{D_s}(\mathbf{q_s})\ddot{\mathbf{q}}_\mathbf{s} + \mathbf{C_s}(\mathbf{q_s}, \dot{\mathbf{q}}_\mathbf{s})\dot{\mathbf{q}}_\mathbf{s} + \mathbf{G_s}(\mathbf{q_s}) = \mathbf{B_s}u, \tag{1}$$

where u is the torque acting on the hip joint, $\mathbf{B_s} = [0\ \ 1\ \ 0]^T$, $\mathbf{G_s}(\mathbf{q_s})$ is a vector related to the total potential energy, $\mathbf{D_s}(\mathbf{q_s})$ and $\mathbf{C_s}(\mathbf{q_s}, \dot{\mathbf{q}}_\mathbf{s})$ are the inertia and the Coriolis matrix, respectively.

Written as a state space model, it is

$$\dot{\mathbf{x}}_\mathbf{s} = \mathbf{f_s}(\mathbf{x_s}) + \mathbf{g_s}(\mathbf{x_s})u \tag{2}$$

where the state is $\mathbf{x_s} = [\mathbf{q}_\mathbf{s}^T\ \ \dot{\mathbf{q}}_\mathbf{s}^T]^T$ and

$$\mathbf{f_s}(\mathbf{x_s}) = \begin{bmatrix} \dot{\mathbf{q}}_\mathbf{s} \\ -\mathbf{D_s^{-1}}(\mathbf{q_s})\left[\mathbf{C_s}(\mathbf{q_s}, \dot{\mathbf{q}}_\mathbf{s})\dot{\mathbf{q}}_\mathbf{s} + \mathbf{G_s}(\mathbf{q_s})\right] \end{bmatrix},$$

$$\mathbf{g_s}(\mathbf{x_s}) = \begin{bmatrix} \mathbf{0_{3\times 1}} \\ \mathbf{D_s^{-1}}(\mathbf{q_s})\mathbf{B_s} \end{bmatrix}.$$

2.2. Flight-phase model

At the flight phase, we denote $\mathbf{q_f} = [q_1\ q_2\ x_{cm}\ y_{cm}]^T$ the generalized coordinates. The equations of motion at the flight phase can be derived by the Lagrangian method as follows

$$\mathbf{D_f}(q_2)\ddot{\mathbf{q}}_\mathbf{f} + \mathbf{C_f}(\mathbf{q_f}, \dot{\mathbf{q}}_\mathbf{f})\dot{\mathbf{q}}_\mathbf{f} + \mathbf{G_f}(\mathbf{q_f}) = \mathbf{B_f}u, \tag{3}$$

where $\mathbf{D_f}(q_2)$, $\mathbf{C_f}(\mathbf{q_f}, \dot{\mathbf{q}}_\mathbf{f})$, and $\mathbf{G_f}(\mathbf{q_f})$ are defined correspondingly, and $\mathbf{B_f} = [0\ 1\ 0\ 0]^T$. Note that $\mathbf{D_f}(q_2)$ depends only on q_2 because the kinetic energy is invariant under rotations and translations of the whole body.

The state space model is then

$$\dot{\mathbf{x}}_\mathbf{f} = \mathbf{f_f}(\mathbf{x_f}) + \mathbf{g_f}(\mathbf{x_f})u \tag{4}$$

https://doi.org/10.1017/S0263574710000512 Published online by Cambridge University Press

where $\mathbf{x_f} = [\mathbf{q_f}^T \ \dot{\mathbf{q}}_\mathbf{f}^T]^T$, and $\mathbf{f_f}(\mathbf{x_f})$ and $\mathbf{g_f}(\mathbf{x_f})$ have the similar forms as at the stance phase.

2.3. State transitions

As mentioned above, a running motion is composed of a series of stance and flight phases. Thus, we must consider the state transition rules between these phases in order to reinitialize the continuous dynamics. We give the takeoff and touchdown models below, which describe the transition from the stance phase to the flight phase and the transition from the flight phase to the stance phase, respectively. In what follows, we use the superscripts $+$ and $-$ to represent the states after and before transitions.

2.3.1. Takeoff model. Takeoff occurs when the deformation length of the spring is zero, i.e., $b - b_0 = 0$. The energy and the linear and angular momentums are conserved before and after takeoff. That is,

$$\begin{bmatrix} q_1^+ \\ q_2^+ \\ \dot{q}_1^+ \\ \dot{q}_2^+ \end{bmatrix} = \begin{bmatrix} q_1^- \\ q_2^- \\ \dot{q}_1^- \\ \dot{q}_2^- \end{bmatrix}. \tag{5}$$

The CoG (x_{cm}, y_{cm}) is related to the mass distribution of the robot and can be expressed in terms of the position (x_t, y_t) of the stance foot and $\mathbf{q_s}$ as follows:

$$\begin{bmatrix} x_{cm} \\ y_{cm} \end{bmatrix} = \begin{bmatrix} x_t \\ y_t \end{bmatrix} + \mathbf{p}(\mathbf{q_s}) \tag{6}$$

where

$$\mathbf{p}(\mathbf{q_s}) = \begin{bmatrix} -\dfrac{(m_H l + m(2l-a))\sin(q_1) - ma\sin(q_1+q_2)}{2m+m_H} \\ \dfrac{(m_H l + m(2l-a))\cos(q_1) - ma\cos(q_1+q_2)}{2m+m_H} \end{bmatrix}.$$

During the stance phase, the stance foot acts as an ideal pivot and thus has zero linear velocity, which yields

$$\begin{bmatrix} \dot{x}_{cm}^+ \\ \dot{y}_{cm}^+ \end{bmatrix} = \begin{bmatrix} \dot{x}_{cm}^- \\ \dot{y}_{cm}^- \end{bmatrix} = \frac{\partial \mathbf{p}(\mathbf{q_s})}{\partial \mathbf{q_s}} \dot{\mathbf{q}}_\mathbf{s}^-. \tag{7}$$

Finally, we can calculate the takeoff model from (5)–(7).

$$\mathbf{x}_\mathbf{f}^+ = \Delta_\mathbf{s}^\mathbf{f}(\mathbf{x}_\mathbf{s}^-). \tag{8}$$

2.3.2. Touchdown model. Touchdown occurs when the height of the touchdown foot above the ground is zero, i.e., $y_t(\mathbf{q_f}) = 0$.

When landing, the touchdown foot acts as an ideal pivot without rebound and slipping and thus has zero linear velocity. From (6), we obtain

$$\begin{bmatrix} 0 \\ 0 \end{bmatrix} = \begin{bmatrix} \dot{x}_{cm}^+ \\ \dot{y}_{cm}^+ \end{bmatrix} - \frac{\partial \mathbf{p}(\mathbf{q_s})}{\partial \mathbf{q_s}} \dot{\mathbf{q}}_\mathbf{s}^+. \tag{9}$$

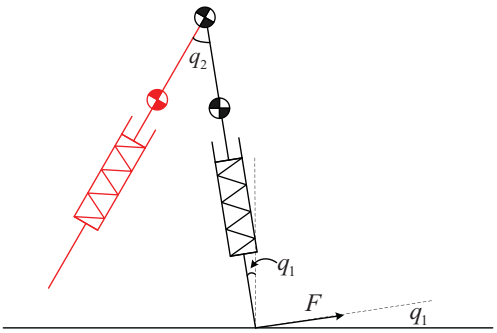


Fig. 3. The impact impulse force at the moment of touchdown.

Since we assume that there is no rebound and no slipping when landing, the touchdown impact results in an instantaneous change of the velocities for the generalized coordinates, but the generalized coordinates remain continuous. In other words, the length of the spring does not instantaneous change when the impact occurs. Hence, the impact impulse force can only take effect along the direction perpendicular to the touchdown leg, which is denoted by F in Fig. 3. Thus, one obtains that

$$\mathbf{D_f}(q_2)(\dot{\mathbf{q}}_\mathbf{f}^+ - \dot{\mathbf{q}}_\mathbf{f}^-) = \begin{bmatrix} -\dfrac{\partial \mathbf{p}(\mathbf{q_s})}{\partial \mathbf{q}} \\ \mathbf{I_{2\times 2}} \end{bmatrix} \begin{bmatrix} F\cos(q_1) \\ F\sin(q_1) \end{bmatrix}, \tag{10}$$

where $\mathbf{q}$ is the first two components of $\mathbf{q_s}$, (i.e., $\mathbf{q} = [q_1 \ q_2]^T$).

Combining (9) and (10) leads to the touchdown model

$$\mathbf{x}_\mathbf{s}^+ = \Delta_\mathbf{f}^\mathbf{s}(\mathbf{x}_\mathbf{f}^-). \tag{11}$$

where $\Delta_\mathbf{f}^\mathbf{s}$ can be calculated from (9) and (10).

The impact model of a running motion is different from that of walking. Due to the springy telescopic legs, it cannot be expressed as two rigid bodies that are used in refs. [2, 9, 30, 34].

2.4. The overall hybrid model

Let $\mathcal{S}_1$ be the set of states $\mathbf{x_s}$ for which the robot takes off, i.e., the spring of the stance leg resumes its uncompressed status and the velocity of the stance foot is directly off the ground. On the other hand, we define $\mathcal{S}_2$ the set of states $\mathbf{x_f}$ for which the robot is going to transit from a flight phase to a stance phase. Thus, the overall model of a running motion is obtained by combining stance, takeoff, flight, and touchdown, which is given by a hybrid system model with multiple continuous state spaces,

$$\sum : \begin{cases} \dot{\mathbf{x}}_\mathbf{s} = \mathbf{f_s}(\mathbf{x_s}) + \mathbf{g_s}(\mathbf{x_s})u, & \\ \mathbf{x}_\mathbf{f}^+ = \Delta_\mathbf{s}^\mathbf{f}(\mathbf{x}_\mathbf{s}^-), & \mathbf{x}_\mathbf{s}^- \in \mathcal{S}_1, \\ \dot{\mathbf{x}}_\mathbf{f} = \mathbf{f_f}(\mathbf{x_f}) + \mathbf{g_f}(\mathbf{x_f})u, & \\ \mathbf{x}_\mathbf{s}^+ = \Delta_\mathbf{f}^\mathbf{s}(\mathbf{x}_\mathbf{f}^-), & \mathbf{x}_\mathbf{f}^- \in \mathcal{S}_2. \end{cases} \tag{12}$$

3. Passive limit cycle

In this section, we look for the condition to preserve the system energy at touchdown and it is expected that the system autonomously generates a natural periodic orbit when the

https://doi.org/10.1017/S0263574710000512 Published online by Cambridge University Press

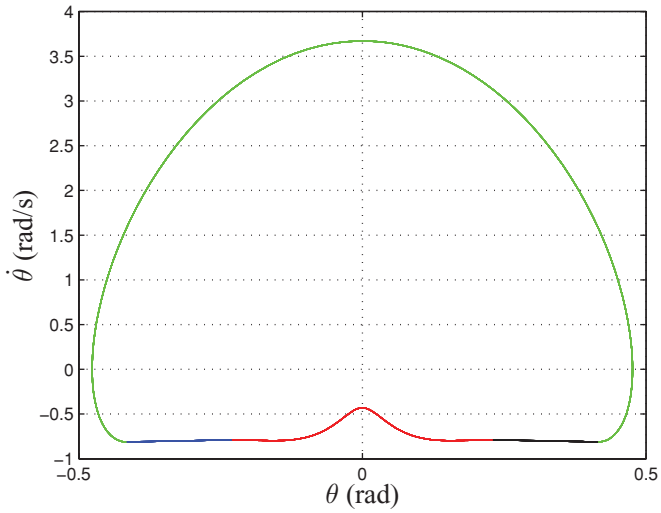


Fig. 4. A passive limit cycle that satisfies the condition of preserving the system energy at touchdown.

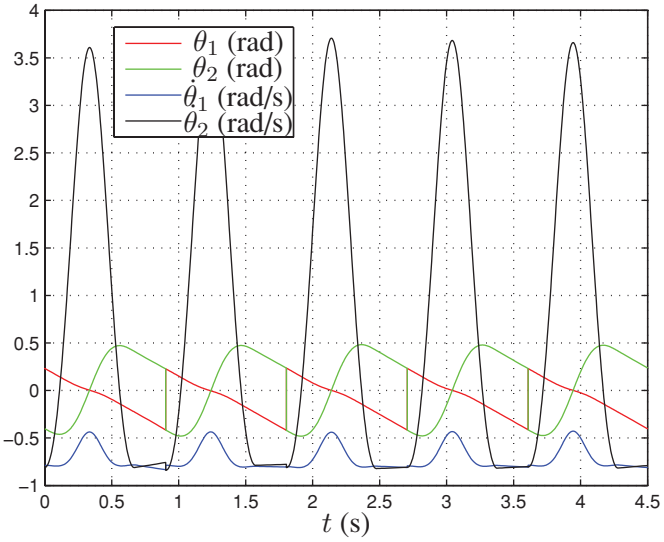


Fig. 5. Periodic trajectories of angles θ_1, θ_2 and angular velocities $\dot{\theta}_1, \dot{\theta}_2$ within five steps.

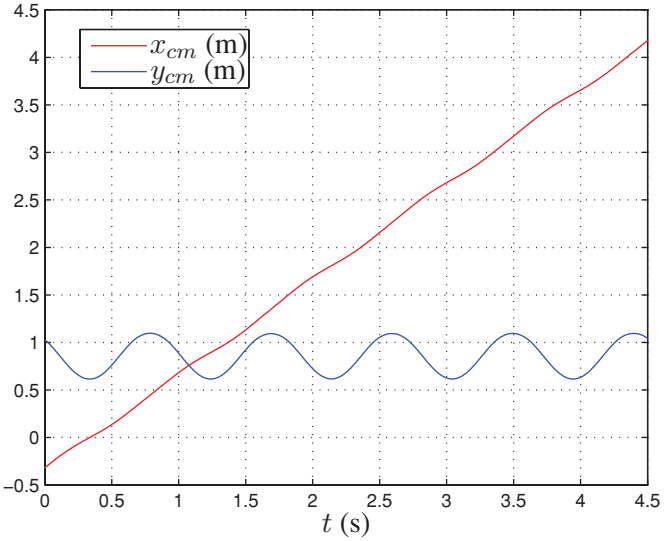


Fig. 6. Periodic trajectories of CoG.

system energy is preserved. In order to preserve the system energy, the reaction force should be zero, which implies $\dot{\mathbf{q}}_\mathbf{f}^+ - \dot{\mathbf{q}}_\mathbf{f}^- = \mathbf{0}$. Combining this condition ($\dot{x}_{cm}$ and $\dot{y}_{cm}$ are the third and fourth components of $\dot{\mathbf{q}}_\mathbf{f}$) and (9), we obtain that

$$\begin{bmatrix} \dot{x}_{cm}^- \\ \dot{y}_{cm}^- \end{bmatrix} = \frac{\partial \mathbf{p}(\mathbf{q_s})}{\partial \mathbf{q}} \dot{\mathbf{q}}^- + \begin{bmatrix} -\sin(q_1) \\ \cos(q_1) \end{bmatrix} \dot{b}^+, \tag{13}$$

where $\mathbf{q}$ is the first two components of $\mathbf{q_s}$ and b is the third component of $\mathbf{q_s}$. Let $p_1(\mathbf{q_s})$ and $p_2(\mathbf{q_s})$ be the first and second component of $\mathbf{p}(\mathbf{q_s})$, respectively. Eliminating $\dot{b}^+$ in (13), we obtain

$$\frac{\dot{x}_{cm}^- - \dfrac{\partial p_1(\mathbf{q_s})}{\partial \mathbf{q}} \dot{\mathbf{q}}^-}{\dot{y}_{cm}^- - \dfrac{\partial p_2(\mathbf{q_s})}{\partial \mathbf{q}} \dot{\mathbf{q}}^-} = \frac{-\sin(q_1)}{\cos(q_1)}, \tag{14}$$

which gives a constraint just before touchdown for energy preservation. It means that the linear velocity of the touchdown foot is consistent with the direction of the touchdown leg. This condition is useful in finding a passive limit cycle.

We use the method of *Poincaré* shooting described in ref. [24] to seek for a passive limit cycle. We select an initial condition satisfying (14) to start the search. For the robot with the parameters given in Table I, a passive limit cycle satisfying the constraint (14) is found and shown in Fig. 4. The passive limit cycle in Fig. 4 is drawn in terms of the variables θ_1, θ_2, and $\dot{\theta}_1$, $\dot{\theta}_2$, where $\theta_1 = q_1$ and $\theta_2 = q_1 + q_2$ that is the angle between the swing leg and the vertical line. The red and green line segment in Fig. 4 corresponds to the stance leg and the swing leg in the stance phase, respectively. The blue and black line segment corresponds to the leg just taking off and the leg going to touch down in the flight phase, respectively. From the figure, we can see that the passive limit cycle is a smooth and closed curve, which implies that the energy is preserved at touchdown.

The periodic evolutions of $\theta_1, \theta_2, \dot{\theta}_1$, and $\dot{\theta}_2$ with respect to the time are shown in Fig. 5. Two legs exchange their roles at the end of each step. Figure 6 depicts the trajectories of the CoG over five steps. The deformation length of the spring and its changing rate over five steps are plotted in Fig. 7. In Fig. 7, the flight phase is the interval during which the deformation length of the spring and its changing rate are both zero, and the stance phase is the rest.

Using the touchdown model, we can calculate the minimum friction coefficient that is required. Running on the passive limit cycle, the friction coefficient μ should satisfy $\mu > \tan(q_1^*) = 0.2342$, where q_1^* is the value of q_1 at the moment of touchdown. The requirement of this friction coefficient is not difficult to be satisfied in practical setup.

4. Stability of Passive Limit Cycle

Cyclic stability is the core concept for limit cycles. In this section, we show that the passive limit cycle is unstable if no control effort is made to stabilize it.

To check the cyclic stability of the passive limit cycle, we select the definite point at the moment of touchdown of every step. Note that at the definite point of each step, $b = b_0$. So,

https://doi.org/10.1017/S0263574710000512 Published online by Cambridge University Press

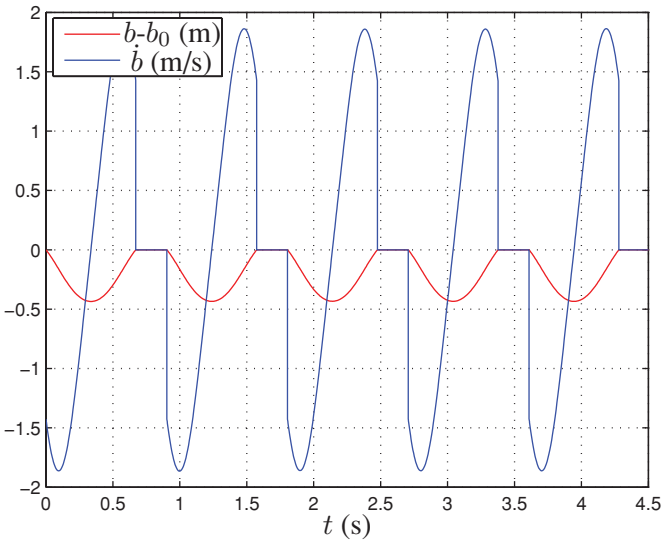


Fig. 7. Periodic evolutions of deformation length of the spring and its changing rate. The deformation length of the spring and its changing rate are both zero at flight phases.

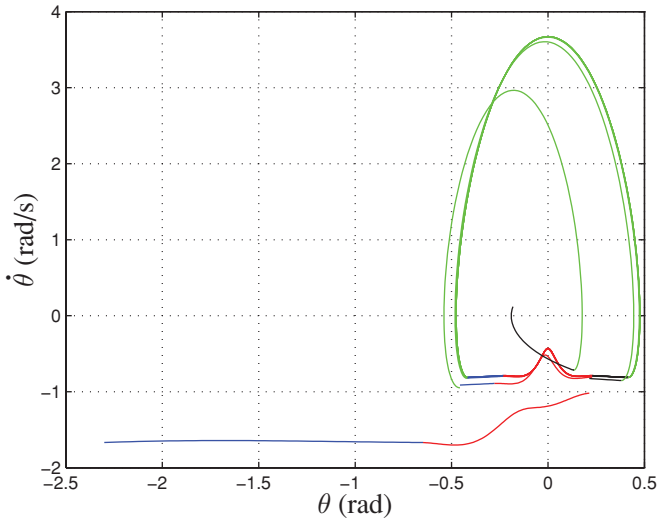


Fig. 8. Even with an initial condition very close to the passive limit cycle, the trajectory diverges and the system without any control is unstable.

we only use $(q_1^+, q_2^+, \dot{q}_1^+, \dot{q}_2^+, \dot{b}^+)$ to represent the state of the robot at the definite point, denoted by $\mathbf{x}$. Then we calculate the *Poincaré* map $\mathbf{P}$, which maps the state of the definite point at current step to the state of the same definite point at next step. Thus, a nonlinear discrete-time system is induced.

$$\mathbf{x}(k+1) = \mathbf{P}(\mathbf{x}(k)). \tag{15}$$

The map $\mathbf{P}$ determined by the dynamic model of a running motion is usually solved numerically. By Matlab, the fixed point satisfying $\mathbf{x}^* = \mathbf{P}(\mathbf{x}^*)$ for our system is

$$\mathbf{x}^* = \begin{bmatrix} 0.230112384058429 \\ -0.645654946390774 \\ -0.788331752652259 \\ -0.023475860503137 \\ -1.425185602239223 \end{bmatrix}.$$

The linearization at $\mathbf{x}^*$ of our system (15) can also be calculated, where the linearized system matrix

$$\mathbf{A} = \begin{bmatrix} 2.512 & -1.109 & 0.926 & -0.511 & 0.167 \\ 2.137 & 0.922 & 1.150 & 0.403 & -0.008 \\ 22.376 & -3.376 & 10.013 & -1.390 & 0.405 \\ -9.817 & 2.226 & -4.125 & 0.956 & -0.269 \\ -18.561 & 4.821 & -8.255 & 1.903 & 0.350 \end{bmatrix}.$$

It can be easily checked that the eigenvalues of A are $\lambda_1 = 11.9354$, $\lambda_2 = 1.7997$, $\lambda_3 = 1.0013$, $\lambda_4 = -0.0426$, and $\lambda_5 = 0.0593$, for which three eigenvalues are outside of the unit circle in the complex plane. Hence, the fixed point $\mathbf{x}^*$ is unstable, meaning that the passive limit cycle is unstable. An unstable trajectory is shown in Fig. 8 even though the initial state is selected to be very close to the passive limit cycle.

5. Event-Based Stabilizing Controller

In this section, we synthesize a feedback control law to stabilize the passive limit cycle. We adopt a method, which is successfully used for stable walking in ref. [6], for our control purpose.

In our setup, there is only one control input u, which is the torque acting on the hip joint. We consider the following control strategy. We let $u(t) = \alpha(k)$ when t is in the interval of the stance phase at the kth step, and let $u(t) = \beta(k)$ when t is in the interval of the flight phase at the kth step, where $\alpha(k)$ and $\beta(k)$ will be designed later depending on the state $\mathbf{x}(k)$ at the definite point of the kth step.

Considering α and β as the inputs, we again calculate the nonlinear system induced from the *Poincaré* map. That is,

$$\mathbf{x}(k+1) = \mathbf{P}(\mathbf{x}(k), \alpha(k), \beta(k)). \tag{16}$$

Linearizing the nonlinear system (16) about the fixed point x^* and the nominal values $\alpha^* = 0$, $\beta^* = 0$ leads to

$$\Delta\mathbf{x}(k+1) = \mathbf{A}\Delta\mathbf{x}(k) + \mathbf{B}\begin{bmatrix} \Delta\alpha(k) \\ \Delta\beta(k) \end{bmatrix}, \tag{17}$$

where $\mathbf{A}$ is the same matrix as defined in the proceeding section and $\mathbf{B}$ is computed numerically in the same way, yielding

$$\mathbf{B} = \begin{bmatrix} -0.0205 & 0.0172 \\ 0.0453 & -0.0298 \\ -0.0079 & 0.0144 \\ 0.2306 & -0.0241 \\ 0.0732 & -0.0881 \end{bmatrix}. \tag{18}$$

Denote $\Delta\mathbf{W} = [\Delta\alpha,\ \Delta\beta]^T$. The DLQR approach is used to design the feedback control of the following form

$$\Delta\mathbf{W}(k) = -\mathbf{K}\Delta\mathbf{x}(k) \tag{19}$$

https://doi.org/10.1017/S0263574710000512 Published online by Cambridge University Press

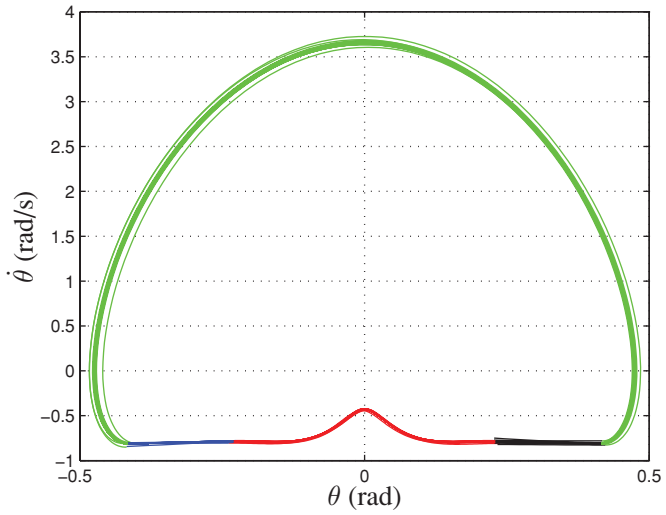


Fig. 9. Converging to the passive limit cycle from an initial state perturbed away from the fixed point.

so that it minimizes the cost function

$$\sum_k \left(\Delta \mathbf{x}^T(k)\mathbf{Q}\Delta \mathbf{x}(k) + \Delta \mathbf{W}^T(k)\mathbf{R}\Delta \mathbf{W}(k)\right).$$

The feedback gain $\mathbf{K}$ is then obtained,

$$\mathbf{K} = \begin{bmatrix} 238.27 & -49.84 & 103.96 & -21.1 & 4.5 \\ -104.52 & 27.27 & -43.18 & 12.2 & -4.9 \end{bmatrix}.$$

It can be checked that with this feedback control law, the closed-loop system becomes stable, indicating that the running limit cycle is stable.

To illustrate the effectiveness of our proposed control law, a simulation is run for 500 steps with the initial angles $q_1(0)$ and $q_2(0)$ (0.1° and 0.5° perturbed away from the fixed-point $\mathbf{x}^*$). The simulated trajectory is given in Fig. 9, from which it is clear that the robot is able to maintain a stable running gait. The step length and the step velocity are shown in Fig. 10 for the first 30 steps, from which it can be seen that they converge to the step length and the step velocity in the passive mode. The control signal $u(t)$ is presented in Fig. 11, where α and β are alternative constants separated by red dot lines.

6. Enlarge the Basin of Attraction

In the preceding section, an event-based feedback controller is devised to stabilize the running orbit to the passive limit cycle. However, the basin of attraction is rather small. In this section, we use passivity-based control to enlarge the basin of attraction and increase additional robustness. The similar idea was used in ref. [30] for stable walking. Now, we change the control law u to be of the following form:

$$u = \bar{u} + u_p, \tag{20}$$

where $\bar{u}$ is the piecewise constant control obtained in the previous section and u_p is a new term to be designed later.

When the robot is in the flight phase, the kinetic energy and the potential energy are not controllable. Consequently, we let $u_p = 0$ in the flight phase.

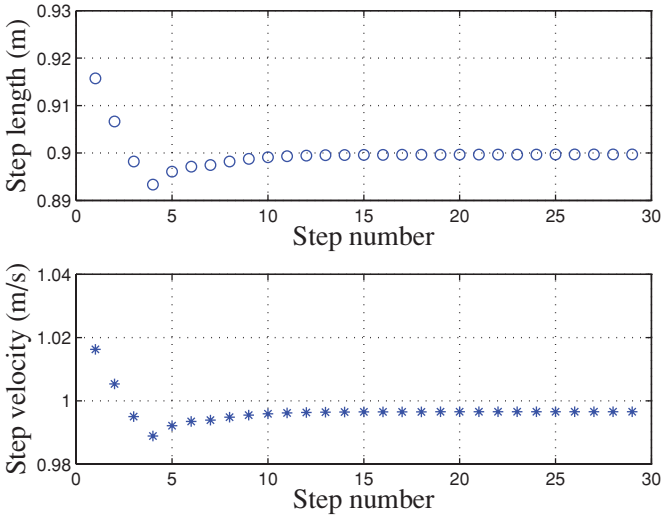


Fig. 10. The step length and the step velocity in the first 30 steps. They tend toward some constant values, which can be calculated from the passive limit cycle.

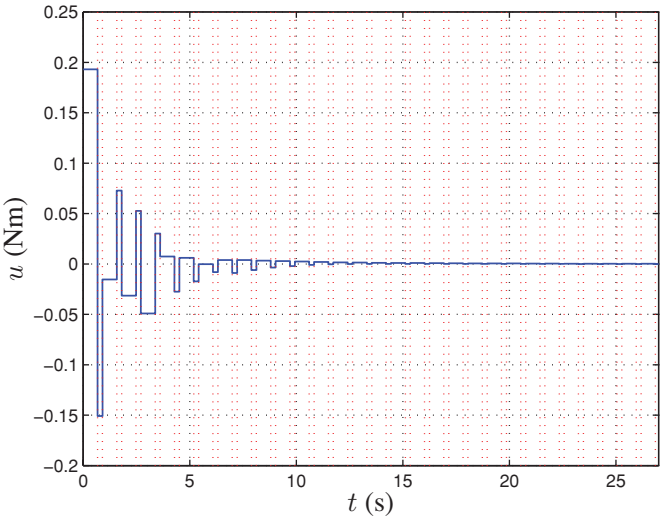


Fig. 11. The applied piecewise constant control input signal where α and β are alternatively shown in the figure separated by the red dotted lines. The control signal tends toward zero.

Note that the dynamic model in the stance phase defines a passive system with the input u and the total energy

$$E = \frac{1}{2}\dot{\mathbf{q}}_\mathbf{s}^\mathbf{T}\mathbf{D}_\mathbf{s}\dot{\mathbf{q}}_\mathbf{s} + V(\mathbf{q}_\mathbf{s}). \tag{21}$$

According to the skew symmetry of $\dot{\mathbf{D}}_\mathbf{s} - \mathbf{2C}_\mathbf{s}$, it follows that

$$\dot{E} = (\mathbf{B}u)^T\dot{\mathbf{q}}_\mathbf{s}. \tag{22}$$

Let E_{ref} be the total energy when the trajectory is the passive limit cycle and take

$$S = \frac{1}{2}(E - E_{ref})^2 \tag{23}$$

as the Lyapunov storage function in the stance phase. Let us temporarily assume that $u = u_p$ in the stance phase. Thus, in order to ensure that the total energy of the robot decreases to

https://doi.org/10.1017/S0263574710000512 Published online by Cambridge University Press

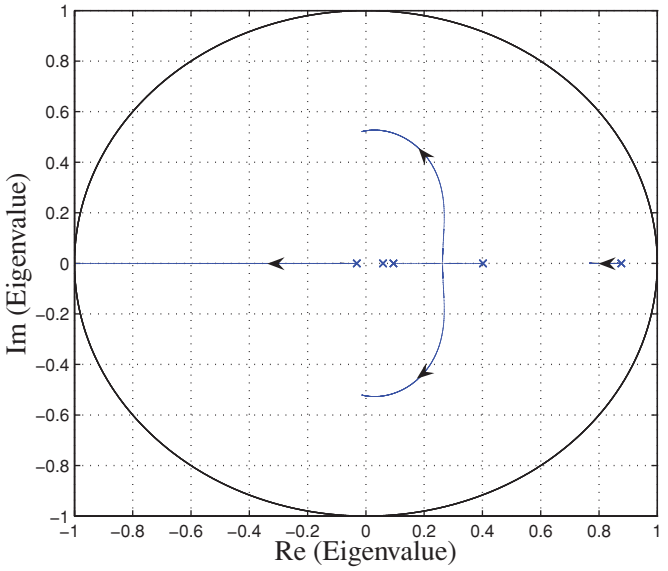


Fig. 12. Root locus of the linearized *Poincaré* map for bipedal running under the control law (20) as the gain k_r varies from 0 to 0.012.

E_{ref}, the control u is chosen as

$$u_p = u = -k_r(E - E_{ref})\dot{q}_2, \tag{24}$$

where $k_r > 0$ is a constant. Thus,

$$\dot{S} = -2k_r\|\dot{q}_2\|^2 S \leq 0. \tag{25}$$

This means that the total energy exponentially converges to E_{ref}, which corresponds to the motion on the passive limit cycle.

For the new control law (20), as now another term u_p is added, we need to check whether the linearized system induced from the *Poincaré* map is still stable. By varying k_r in (24) from 0 to 0.012, the root locus are shown in Fig. 12, and it can be known that the passive limit cycle is still stable as all the eigenvalues are located inside the unit circle.

Next, we numerically compute the basin of attraction and make a comparison for the controllers with and without the new term u_p. For $k_r = 0.01$ in (24), the basins of attraction in the plane of Δq_1, Δq_2 and in the plane of $\Delta\dot{q}_1$, $\Delta\dot{q}_2$ are the gray areas in Figs. 13 and 14, respectively, while the black areas in both figures are the basin of attraction under the control law without the term u_p. It is observed that the basin of attraction with an additional passivity-based control is much larger than that without an additional passivity-based control and the former fully contains the latter.

Consider an initial state where $q_1(0)$ is 0.5° away and $q_2(0)$ is 2.5° away from the fixed point. When we only apply the event-based feedback control law developed in the preceding section, the simulated trajectory shows that the robot cannot maintain a stable running gait. However, when we apply the control law (20), the trajectory converges to the passive limit cycle, which is shown in Fig. 15. In addition, the step length and the step velocity are presented in Fig. 16 for the first 80 steps, and Fig. 17 shows the control signal applied to make a stable running.

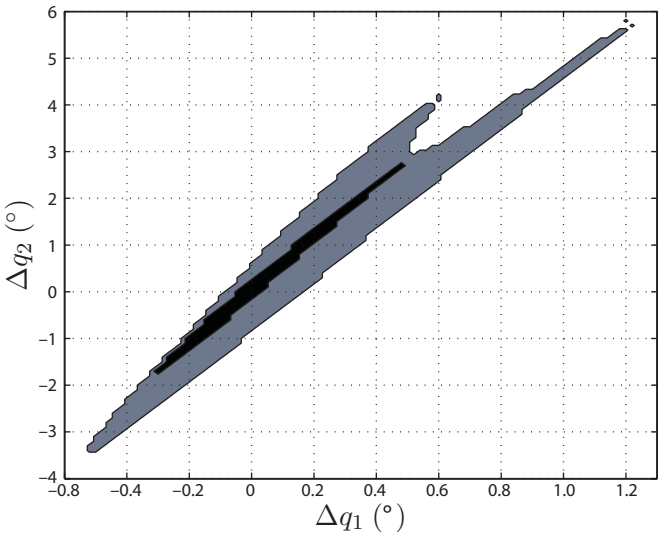


Fig. 13. The gray region is the basin of attraction in the plane of Δq_1, Δq_2 for the robot with an additional passivity-based control term, while the black region is the one for the robot without this additional term.

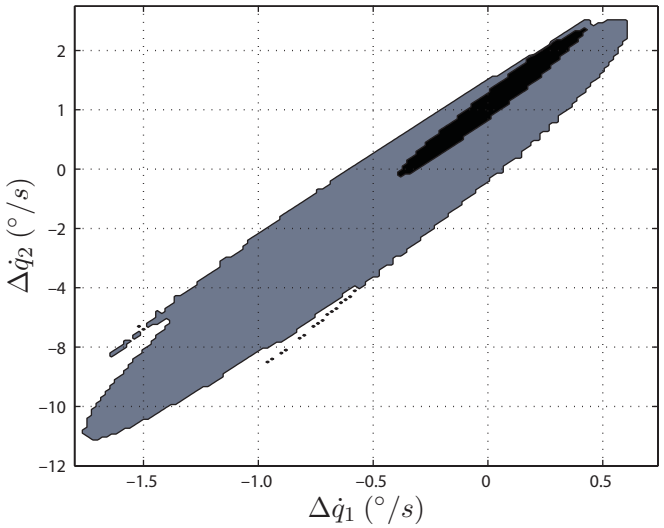


Fig. 14. The gray region is the basin of attraction in the plane of $\Delta\dot{q}_1$, $\Delta\dot{q}_2$ for the robot with an additional passivity-based control term, while the black region is the one for the robot without this additional term.

7. Conclusion

In this paper, the stable running problem of a planar underactuated biped robot is investigated. We explored the conditions that preserve the system energy at touchdown and then used this condition to search for a natural passive limit cycle by the method of *Poincaré* shooting. For the passive limit cycle we found, it is shown that the passive limit cycle is not stable. As a result, an event-based feedback control law is proposed to stabilize the passive limit cycle. Moreover, a passivity-based control term only valid in the stance phase is devised in order to enlarge the basin of attraction and increase the robustness. Stable running on the flat surface is thus achieved under our proposed control law. When the running gait of the robot is exactly the passive limit cycle, no energy is consumed.

https://doi.org/10.1017/S0263574710000512 Published online by Cambridge University Press

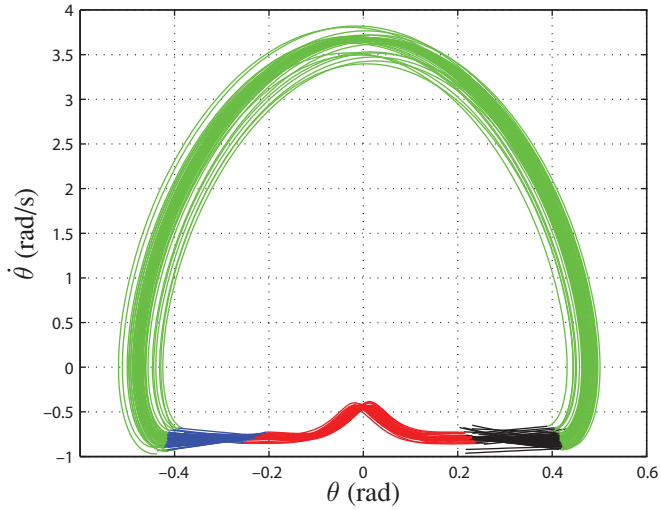


Fig. 15. Stable running under the control law (20). The simulated trajectory tends toward the passive limit cycle from an initial state perturbed away from the fixed point.

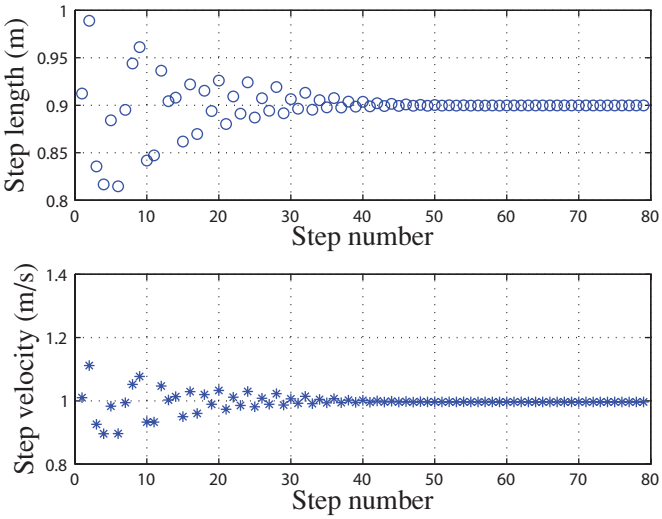


Fig. 16. The step length and the step velocity in the first 80 steps. They tend toward some constants.

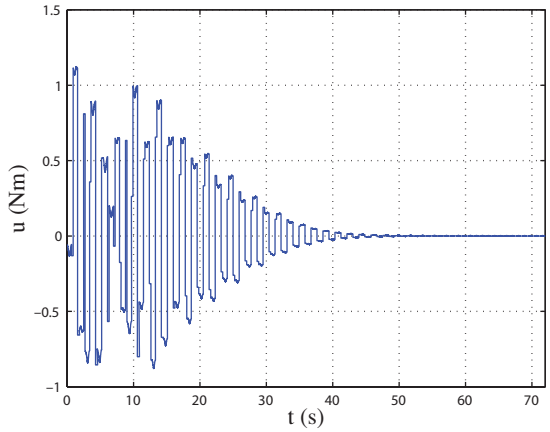


Fig. 17. The convergence of control signal toward zero is observed with the proposed control law (20). The response is presented for the first 80 steps.

The running robot model studied in the paper is planar and rather simple. Extending to 3D running robot model realizing passive running gaits is very important. To do so, a torso with two degree-of-freedom actuation might be needed. On the other hand, enlarging the basin of attraction and gluing together partial solutions for 2D passive running so as to obtain a more satisfying overall solution for 3D running robots are very interesting and promising research subjects.

References

1. A. D. Ames, R. D. Gregg, E. D. B. Wendel and S. Sastry, "On the geometric reduction of controlled three-dimensional bipedal robotic walkers," *Lecture Notes Control Inf. Sci.* **366**, 183–196 (2007).
2. E. Borzova and Y. Hurmuzlu, "Passively walking of five-link robot," *Automatica* **40**(4), 621–629 (2004).
3. M. Buehler and D. E. Koditschek, "Analysis of a simplified hopping robot," *Int. J. Robot. Res.* **10**, 587–605 (1991).
4. C. Chevallereau, G. Abba, Y. Aoustin, F. Plestan, E. R. Westervelt, C. Canudas-de Wit and J. W. Grizzle, "Rabbit: a testbed for advanced control theory," *IEEE Control Syst. Mag.* **23**, 57–79 (2003).
5. C. Chevallereau and Y. Aoustin, "Optimal reference trajectories for walking and running of a biped robot," *Robotica* **19**, 557–569 (2001).
6. C. Chevallereau, J. W. Grizzle and C. Shih, "Asymptotically stable walking of a five-link underactuated 3d bipedal robot," *IEEE Trans. Robot. Autom.* **25**, 37–50 (2008).
7. C. Chevallereau and P. Sardain, "Design and Actuation Optimization of a 4 Axes Biped Robot for Walking and Running." *Proceedings of IEEE International Conference on Robotics and Automation*, San Francisco, USA (2000) pp. 3365–3370.
8. C. Chevallereau, E. R. Westervelt and J. W. Grizzle, "Asymptotic Stabilization of a Five-Link, Four-Actuator, Planar Bipedal Runner," *Proceedings of 43rd IEEE Conference on Decision and Control*, Nassau, Bahamas (2004) pp. 303–310.
9. C. Chevallereau, E. R. Westervelt and J. W. Grizzle, "Asymptotically stable running for a five-link, four-actuator, planar bipedal robot," *Int. J. Robot. Res.* **24**, 431–464 (2005).
10. B. Chu, D. Hong, J. Park and J. H. Chung, "Passive dynamic walker controller design employing an RLS-based natural actor–critic learning algorithm," *Eng. Appl Artif. Intell.* **21**, 1027–1034 (2008).
11. S. Collins, A. Ruina, R. Tedrake and M. Wisse, "Efficient bipedal robots based on passive-dynamic walkers," *Science* **307**, 1082–1085 (2005).
12. M. Garcia, A. Chatterjee, A. Ruina and M. Coleman, "The simplest walking model: Stability, complexity and scaling," *J. Biomech. Eng.* **120**, 281–288 (1998).
13. L. Geppert, "QRIO, the robot that could." *IEEE Spectr.* **41**, 34–37 (2004).
14. A. Goswami, B. Thuilot and B. Espiau, "A study of the passive gait of a compass-like biped robot: symmetry and chaos," *Int. J. Robot. Res.* **17**, 1282–1311 (1998).
15. R. Hirose and T. Takenaka, "Development of the humanoid robot ASIMO," *Honda R&D Tech. Rev.* **13**, 1–6 (2001).
16. S. H. Hyon and T. Emura, "Running Control of a Planar Biped Robot Based on Energy-Preserving Strategy," *Proceedings of IEEE International Conference on Robotics and Automation*, New Orleans, USA (2004) pp. 3791–3796.
17. T. Ishida, "Development of a Small Biped Entertainment Robot QRIO," *Proceedings of the 2004 International Symposium on Micro-NanoMechatronics and Human Science*, Nagoya, Japan (2004), pp. 23–28.
18. K. Kaneko, F. Kanehiro, S. Kajita, H. Hirukawa, T. Kawasaki, M. Hirata, K. Akachi and T. Isozumi, "Humanoid Robot HRP-2," *Proceedings of 2004 IEEE International Conference on*

https://doi.org/10.1017/S0263574710000512 Published online by Cambridge University Press

Robotics and Automation, New Orleans, USA (2004) pp. 1083–1090.
19. T. McGeer, "Passive Bipedal Running," *Proceedings of the Royal Society of London. Series B, Biological Sciences*, The Royal Society (1990) pp. 107–134.
20. T. McGeer, "Passive dynamic walking," *Int. J. Robot. Res.* **9**, 62–82 (1990).
21. B. Morris, E. R. Westervelt, C. Chevallereau, G. Buche and J. W. Grizzle, "Achieving bipedal running with RABBIT: six steps toward infinity," *Lecture Notes Control Inf. Sci.* **340**, 277–297 (2006).
22. D. Owaki and A. Ishiguro, "Enhancing Stability of a Passive Dynamic Running Biped by Exploiting a Nonlinear Spring. *IEEE/RSJ International Conference on Intelligent Robots and Systems*, Beijing, China (2006) pp. 4923–4928.
23. D. Owaki, K. Osuka and A. Ishiguro, "On the Embodiment that Enables Passive Dynamic Bipedal Running," *Proceedings of 2008 IEEE International Conference on Robotics and Automation*, Psadena, USA (2008).
24. T. S. Parker and L. O. Chua, *Practical Numerical Algorithms for Chaotic Systems* (Springer-Verlag, 1989).
25. I. Poulakakis, E. Papadopoulos and M. Buehler, "On the stability of the passive dynamics of quadrupedal running with a bounding gait," *Int. J. Robot. Res.* **25**, 669–687 (2006).
26. M. H. Raibert, *Legged Robots That Balance* (The MIT Press, 1986).
27. M. H. Raibert and E. R. Tello, "Legged robots that balance," *IEEE Expert [see also IEEE Intelligent Systems and Their Applications]* **1**, 89–89 (1986).
28. A. Sato and M. Buehler, "A Planar Hopping Robot with one Actuator: Design, Simulation and Experimental Results. *Proceedings of 2004 IEEE/RSJ International Conference on Intelligent Robots and Systems*, Sendai, Japan (2004) pp. 3540–3545.
29. S. Satoshi, F. Katsuhisa and H. Shoshiro, "Passive walking towards running," *Math. Comput. Modelling Dyn. Syst.* **11**, 371–395 (2005).
30. M. W. Spong, J. K. Holm and D. Lee, "Passivity-based control of bipedal locomotion," *IEEE Robot. Autom. Mag.* **14**, 30–40 (2007).
31. R. Tedrake, T. W. Zhang, M. Fong and H. S. Seung, "Actuating a Simple 3D Passive Dynamic Walker," *Proceedings of 2004 IEEE International Conference on Robotics and Automation*, New Orleans, USA (2004) pp. 4656–4661.
32. A. F. Vakakis and J. W. Burdick, "Chaotic Motions in the Dynamics of a Hopping Robot," *Proceedings of 1990 IEEE International Conference on Robotics and Automation*, Tsukuba, Japan (1990) pp. 1464–1469.
33. E. R. Westervelt, J. W. Grizzle, C. Chevallereau, J. H. Choi and B. Morris, *Feedback Control of Dynamic Bipedal Robot Locomotion* (CRC Press, 2007).
34. M. Wisse, G. Feliksdal, J. Van Frankkenhuyzen and B. Moyer, "Passive-based walking robot," *IEEE Robot. Autom. Mag.* **14**, 52–62 (2007).

https://doi.org/10.1017/S0263574710000512 Published online by Cambridge University Press